Triplet Excimer Emission in a Series of 4,4′-Bis(*N*-carbazolyl)-2,2′-biphenyl Derivatives

S. T. Hoffmann,[†] P. Schrögel,[‡] M. Rothmann,[‡] R. Q. Albuquerque,[†] P. Strohriegl,[‡] and A. Köhler*,[†]

Experimentalphysik II and Makromolekulare Chemie I, Universität Bayreuth, 95440 Bayreuth, Germany

Received: August 6, 2010; Revised Manuscript Received: November 17, 2010

Carbazole-based materials such as 4,4′-bis(*N*-carbazolyl)-2,2′-biphenyl (CBP) and its derivatives are frequently used as matrix materials for phosphorescent emitters in organic light emitting diodes (OLED)s. An essential requirement for such matrix materials is a high energy of their first triplet excited state. Here we present a detailed spectroscopic investigation supported by density functional theory (DFT) calculations on two series of CBP derivatives, where CH_3 and CF_3 substituents on the 2- and 2′-position of the biphenyl introduce strong torsion into the molecular structure. We find that the resulting poor coupling between the two halves of the molecules leads to an electronic structure similar to that of *N*-phenyl-3,6-dimethylcarbazole, with a high triplet-state energy of 2.95 eV. However, we also observe a triplet excimer emission centered at about 2.5−2.6 eV in all compounds. We associate this triplet excimer with a sandwich geometry of neighboring carbazole moieties. For compounds with the more polar CF_3 substituents, the lifetime of the intermolecular triplet excited state extends into the millisecond range for neat films at room temperature. We attribute this to an increased charge-transfer character of the intermolecular excited state for the more polar substituents.

Introduction

While organic semiconductor materials are of current interest for a range of applications such as solar cells, displays, sensing, or radio frequency identification tags (RFIDs),[1] they offer particularly promising opportunities for solid-state lighting since they allow for the engineering of efficient white organic light emitting devices (WOLEDs).[2,3] One approach to WOLEDs consists in the use of red, green, and blue emissive dopants that are incorporated into carefully designed multilayer structures or suitably attached as side groups to a polymer backbone.[2−4] As an alternative method, the incorporation of a single emitter with efficient broad excimer emission has been demonstrated successfully.[5] In either case, the emitters used in WOLEDs require host materials that need to fulfill several constraints. To allow for efficient charge injection from both electrodes, the energy separating the highest occupied molecular orbital (HOMO) and the lowest unoccupied molecular orbital (LUMO) should be not too high. At the same time, the energy of the first triplet excited state needs to be high enough so that phosphorescence from blue or green emitters is not quenched by energy transfer to the host.

Host materials that are considered suitable and that are therefore used frequently for WOLED applications are often based on carbazole structures,[5−9] such as CBP (CBP = 4,4′-bis(9-carbazolyl)biphenyl) or poly(vinylcarbazole)-like polymers.[10−15] Approaches to obtain high triplet energies include reducing the size of the conjugated system, e.g., by replacing the biphenyl bridging between the two carbazoles with a single phenyl as in mCP (mCP = 3,5-bis(9-carbazolyl)benzene),[16] or by introducing torsion between the two biphenyls as in 4,4′-bis(9-carbazolyl)-2,2′-dimethylbiphenyl (CDBP).[7] This substitution leads to good results with respect to emission and efficiency. We have recently reported the synthesis of a set of CBP derivatives with triplet excited state energies of about 2.95 eV.[17] As for CDPB, the high triplet energy is obtained by introducing torsion between the biphenyls through substitution with a CH_3 group or a CF_3 group. Further substitution with CH_3 groups on the carbazole moiety was employed to fine-tune HOMO and LUMO levels for optimized charge injection.

We present here a detailed spectroscopic and quantum mechanical study on the electronic structure of these compounds, focusing on the influence of the electron-richer CH_3 group compared to the electron-withdrawing CF_3 group on the nature of the optical transitions. In addition to fluorescence and phosphorescence from the monomer, we observe phosphorescence that can be attributed to a sandwich excimer of adjacent carbazole moieties. While this intermolecular triplet-state emission is present for both types of compounds, the radiative excimer emission rate is higher for the CH_3-substituted compounds than for the compounds with the more polar CF_3 group, where the intermolecular excited state seems to acquire a stronger charge-transfer component. With a view to the ubiquitous use of CBP derivatives as hosts for WOLED applications we note that the well-known propensity of this general class of materials to form excimer states (and the polarity dependence of triplet excimer formation) deserves more attention.[11,18−28] The presence of poorly emissive triplet excimers by the host can easily go unnoticed, in particular when combined with efficient phosphorescent emitters that cover a broad spectral range as is the case in WOLEDs. Nevertheless, long-lived triplet excimers may present nonradiative decay channels, and they can reduce device efficiency and device lifetime if not suitably managed. On the other hand, when the radiative decay rate of the host triplet excimer is high enough, they could be contemplated as emitter materials for WOLEDs by themselves. In the context of the study presented here, we focus on understanding the electronic structure of the CBP derivatives by spectroscopic studies in combination with quantum chemical calculations.

Experimental Section

The series of CBP derivatives were synthesized as described by Schrögel and co-workers.[17] For optical measurements, 10^{-5}

* To whom correspondence should be addressed. E-mail: anna.koehler@uni-bayreuth.de.
[†] Experimentalphysik II.
[‡] Makromolekulare Chemie I.

10.1021/jp107408e
Published on Web 12/28/2010

	CBP	1 (CDBP)	2	3	4	5	6
R_1	H	H	CH_3	CH_3	H	CH_3	CH_3
R_2	H	H	H	CH_3	H	H	CH_3
R_3	H	CH_3	CH_3	CH_3	CF_3	CF_3	CF_3

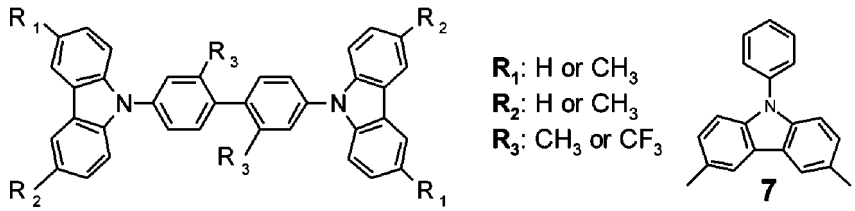

Figure 1. Chemical structures of 4,4′-bis(9-carbazolyl)biphenyl (CBP), the substituted derivatives **1**−**6** and of *N*-phenyl-3,6-dimethylcarbazole (compound **7**).

M cyclohexane solutions of the materials as well as thin films on quartz substrates were prepared. Both neat films and films with 10 wt % of compound in poly(methyl methacrylate) (PMMA) were prepared by spin coating. The ultraviolet−visible (UV/vis) absorption spectra were measured in solution and on neat films with a Hitachi U-3000 spectrometer. Room-temperature steady-state emission spectra from solution and from thin films were obtained from a Shimadzu spectrofluorophotometer RF-5301PC using excitation at 300 nm.

The phosphorescence spectra were taken with the thin film samples mounted in a continuous flow helium cryostat. The temperature was controlled with an Oxford Intelligent temperature controller-4 (ITC-502). Excitation was provided by a pulsed, frequency-tripled Nd:YAG laser at 355 nm (3.49 eV; Spectron SL401). This wavelength corresponds to the red tail of the first absorption band in our compounds. The duration of the laser pulses was 6 ns, and the laser was operated at a repetition rate of 10 Hz by a self-made electronic delay generator. The light emitted by the sample was dispersed and subsequently detected by a time gated intensified CCD camera (Andor iStar DH734-18F-9AM). The measurements were taken with a delay time of 500 ns and a gate width of 60 ms. The measurements were carried out at an excitation density of about 250 μJ cm^{-2} pulse^{-1} on films of about 150 nm thickness as determined by a Dektak profilometer. To increase the signal-to-noise-ratio, all spectra were obtained by averaging over 2000 laser shots.

Density functional theory (DFT) calculations were carried out for compounds **3** and **6** using the B3LYP hybrid functional together with the basis set 6-31G*.[29,30] The excited states were calculated by using time-dependent-DFT with the optimized ground-state geometries. All DFT calculations were carried out with the Gaussian 03 program.

Results and Discussion

(i) Absorption and Fluorescence. We use the widely employed CBP as our reference compound. Figure 1 shows the general structure of the compounds along with a table that details the substitution pattern. To obtain torsion, the 2- and 2′-positions of the biphenyl unit were substituted with electron-withdrawing CF_3 groups or with electron-rich CH_3 moieties. To assess the degree of electronic decoupling obtained by torsion, we compare our materials to *N*-phenyl-3,6-dimethylcarbazole. The structure for *N*-phenyl-3,6-dimethylcarbazole is also displayed in Figure 1. To block the reactive 3- and 6-positions of the carbazole unit, methyl groups have been introduced. In addition, this leads to a further fine-tuning of the electronic structure. Thus, compounds **1**−**6** form two sets of materials, with the group formed by **1** (CDBP), **2**, and **3** based on the methyl-substituted biphenyl center and compounds **4**−**6** based on the trifluoromethyl-substituted core. Within each set, the amount of CH_3 substitution on the carbazole unit rises.

To understand how the substitutions affect the excited states of these compounds, we first consider the effect of torsion by comparing the compounds CBP and CDBP. CDBP differs from CBP only by the presence of the methyl group at the 2,2′-positions of the central biphenyl unit. According to DFT calculations, the methyl group increases the ground-state torsion angle between the two central phenyl rings from about 33 to 81°.[17] Parts a and b of Figure 2 display the room-temperature absorption and fluorescence spectra taken from 10^{-5} M cyclohexane solutions of both compounds. Despite the different ground-state geometries, both CBP and CDBP display a first absorption band at the same energy, that is, with a $S_1 \leftarrow S_0$ 0−0 peak at 3.70 eV and the 0−1 vibrational replica at 3.88 eV, yet for the more planar CBP the molar extinction of this first band is more than twice that found for CDBP. In contrast to CDBP, there is also some intensity at 3.95 eV in CBP. The next absorption band with a 0−0 peak at 4.30 eV and a 0−1 vibrational sideband at 4.45 eV is at the same energy and at very similar intensity for both compounds.

When considering the absorption spectrum of CDBP, we note a striking similarity to the absorption of *N*-phenyl-3,6-dimethylcarbazole that is also displayed in Figure 2 for ease of comparison. In the same way, the fluorescence spectra of *N*-phenyl-3,6-dimethylcarbazole and CDBP coincide. In contrast to the absorption, the emission of CBP is red-shifted compared to CDBP. We attribute this to the planarization of CBP after the transition to the excited state, while such a geometric relaxation is not possible for CDBP due to the bulkier side groups. From this comparison of the three compounds it is evident that the torsion induced by the methyl unit at the central biphenyl reduces conjugation between the two parts of the molecule such that the optical transitions in CDBP are dominated by just the separate *N*-phenylcarbazole moieties.

If the biphenyl is substituted with the electron-withdrawing trifluoromethyl group instead of the electron-rich methyl unit, we observe only minor changes in the absorption yet an entirely

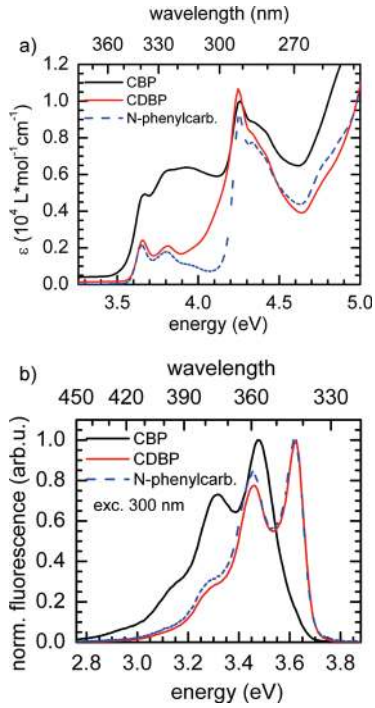

Figure 2. (a) Absorption spectra and (b) fluorescence spectra, both taken at room temperature for CBP, CDBP, and the *N*-phenyl-3,6-dimethylcarbazole **7** in 10^{-5} M cyclohexane solution.

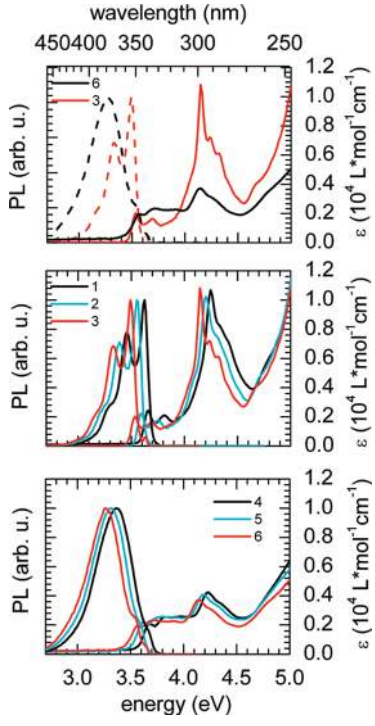

Figure 3. Room-temperature absorption and fluorescence spectra in 10^{-5} M cyclohexane solution (a) for compounds **6** and **3**, (b) for the CH_3-substituted compounds **1**−**3**, and (c) for the CF_3 substituted compounds **4**−**6**.

different spectrum in emission. For example, the only differences in the absorption of compounds **3** and **6** (Figure 3a) are a slightly higher extinction at about 3.85 eV and a significantly reduced extinction in the band around 4 eV for the CF_3-substituted compound while the energetic positions and spectral shapes of the absorption features remain essentially unaltered. In contrast, in the fluorescence spectra the emission energy and vibrational structure differ strongly. The emission of compound **3** closely

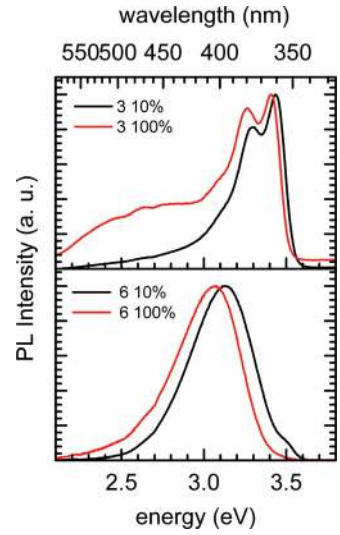

Figure 4. Room-temperature steady-state emission spectra of neat films (labeled 100%) and solid-state solution in PMMA (labeled 10%) normalized to unity (a) for the CH_3-substituted compound **3** and (b) for the CF_3-substituted compound **6**.

resembles that of the parent molecule CBP in both energy and structure, while the luminescence of **6** consists of a broad unstructured peak centered at about 3.25 eV with a small shoulder at 3.55 eV.

Before considering the difference between the CF_3- and the CH_3-substituted compounds in more detail, we briefly comment on the minor modifications to the excited-state energies obtained by introducing additional methyl substituents at the pendant carbazole moieties. We consider compounds **1**−**3** (Figure 3b). For all compounds, we observe a small bathochromic shift with an increasing amount of methyl substituents. Otherwise the spectra retain the features of the carbazole emission. We attribute this to a slight upshift of the HOMO due to the electron-donating character of the methyl group, as confirmed by quantum chemical calculations. The same effect occurs in the trifluoromethyl series **4**−**6** upon CH_3 substitution on the carbazole moiety.

To understand what causes the striking difference in the emission spectra of the CF_3-substituted series compared to the CH_3-substituted one, we compare solution spectra with spectra taken on thin films. The fluorescence spectra taken from the liquid solution (10^{-5} M of the host compound in cyclohexane) are, apart from a very minor bathochromic shift of 50 meV, identical to those taken from thin films of solid-state solution (10 wt % of host compound in PMMA). For the neat films, however, we observe an additional broad emission feature in the CH_3-substituted compound **3** centered at about 2.6 eV. (Figure 4) Such a broad red emission that only occurs in the neat film yet not in solutions is typical for an intermolecular excited state. If we correct for the slight energy shift between the solid solution spectrum and the neat spectrum and then form the difference spectrum between the two, we find that the broad emission centered at 2.6 eV contributes about 40% to the overall neat film emission in **3**. In contrast for **6**, the same red emission only becomes evident after forming the difference spectrum as it amounts to merely 7% of the integrated neat film emission.

We carried out DFT calculations of the molecular orbitals and excited-state energies for the compounds **3** and **6** in order to understand the influence of CF_3 substitution on the central biphenyl compared to the CH_3 substitution. The HOMO and LUMO electron densities are displayed in Figure 5, and the resulting term scheme is shown in Figure 6.

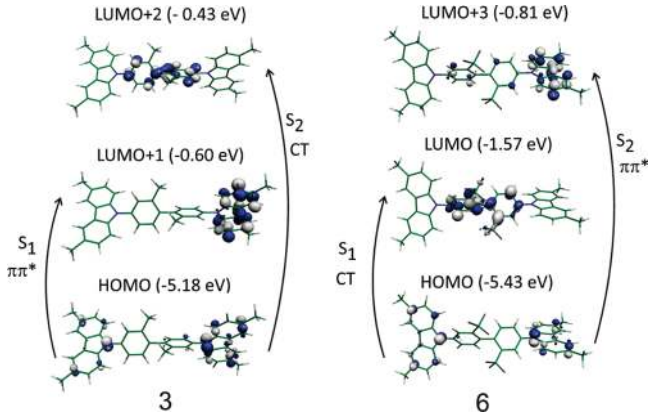

Figure 5. DFT optimized chemical structures and relevant orbitals for compounds **3** (left side) and **6** (right side). The energies of the orbitals with respect to the vacuum level are also indicated. The arrows indicate the transitions into S_1 and S_2 along with their dominant character.

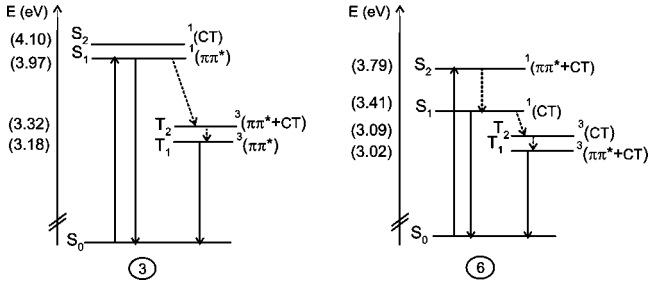

Figure 6. Scheme of the singlet and triplet energy levels based on the DFT calculations for compounds **3** and **6**. The predominant nature of the transitions involved, i.e., charge transfer (CT) or $\pi\pi^*$, is indicated next to the energy levels.

For compound **3**, the torsion between the central biphenyl ring due to the CH_3 groups leads to a localization of the electron wave function on each of the carbazole units. As a result, HOMO and HOMO-1, as well as LUMO and LUMO+1, are nearly degenerate, separated by only 1−2 meV. The lowest excited singlet state, S_1, involves mainly transitions from HOMO→LUMO+1 and HOMO→LUMO. Only the former of the two is illustrated in Figure 6. In the HOMO, the lone pair on the nitrogen mixes with the π-conjugated system of the rings. The transitions contributing to S_1 have predominantly a $\pi\rightarrow\pi^*$ character, and the vertical transition energy is calculated to be at 3.97 eV. At slightly higher energy, that is, at 4.10 eV, we find the second excited singlet state which involves transitions from orbitals localized on the carbazole unit to an orbital localized on the central biphenyl section of the molecule, such as the HOMO→LUMO+2 transition illustrated in Figure 5. S_2 has thus a strong charge-transfer character.

In contrast to **3**, compound **6** is substituted with electron-withdrawing CF_3 groups on the biphenyl. As a result, the orbital localized on the central biphenyl is stabilized and becomes the LUMO. LUMO+1 and LUMO+2 are also centered on the biphenyl. Only orbitals from LUMO+3 onward contain some nonnegligible electron density on the carbazole units. Transitions from a HOMO localized on the carbazole to the LUMO on the biphenyl group lead to a singlet excited state with a strong intramolecular charge-transfer character (and concomitantly a very small oscillator strength) at a vertical transition energy of 3.41 eV. The second excited singlet state S_2 comprises both carbazole−carbazole centered $\pi\rightarrow\pi^*$ transitions such as HOMO →LUMO+3 and carbazole−biphenyl charge-transfer-type transitions. With 3.79 eV, it is at energy similar to the $\pi\rightarrow\pi^*$ based S_1 state in **3**.

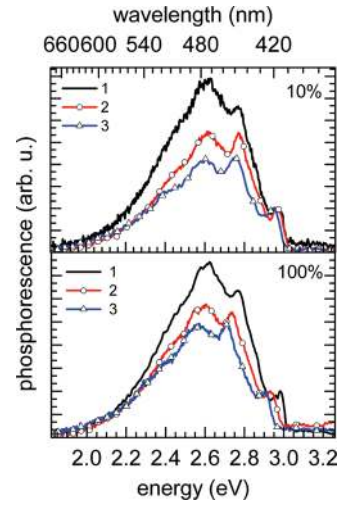

Figure 7. Emission spectra taken at 10 K with a delay time of 500 ns and a gate width of 60 ms for the CH_3-substituted compounds **1**−**3** (a) in a 10 wt % solid-state solution of PMMA and (b) in pure film.The spectra are normalized to unity at the first emission peak.

With these calculations, we can now interpret the absorption and fluorescence spectra. Absorption requires reasonable oscillator strength. Consequently, the absorption observed experimentally at 3.54 eV takes place into the S_1 state of **3** and into the S_2 state of **6**. The S_1 state of **6** cannot be seen in the absorption spectrum due to the low oscillator strength associated with this intramolecular charge-transfer-type transition. After absorption, fluorescence in **3** occurs from the same S_1 state that has been excited, resulting in a small Stokes' shift and clear vibrational structure that mirrors the absorption band (see Figure 3a). In contrast for **6**, fast internal conversion to the lower energy S_1 takes place, in agreement with Kasha's rule.[31] The intramolecular charge-transfer character of the $S_1\rightarrow S_0$ transition precludes a vibrational structure and causes the broad emission.

(ii) Phosphorescence. To experimentally observe the triplet-state emission, we measured the 10 K luminescence from thin films at a delay time of 500 ns after an excitation pulse and using a detector with a large gate width of 60 ms. Figure 7 shows the spectra obtained for **1**−**3**, normalized to unity at about 2.95 eV. The corresponding spectra for **4**−**6** are displayed in Figure 8.

For all spectra taken in a solid-state solution (Figures 7a and 8a), we observe two sharp peaks at 2.95 and at 2.76 eV as well as a broad peak centered at 2.6 eV. The intensity of this broad peak reduces when the number of methyl substituents on the pendant carbazoles is increased along the series **1**−**3** and along the series **4**−**6**.

Increasing the concentration by using a pure film of compounds (Figures 7b and 8b) does not change the spectral shape any further for the series with the methyl substituents on the biphenyl, except for a small bathochromic shift with increasing CH_3 content. In contrast, for the compounds with CF_3 at the central biphenyl, the sharp features are lost and the emission is entirely dominated by the broad peak now centered at 2.5 eV. Furthermore, the spectra do not change with an increasing amount of CH_3 content, except again for a small bathochromic shift.

We consider that the broad peak may be associated with intermolecular interactions since it reduces in relative intensity when the molecule is in a solid solution (compare Figure 8b

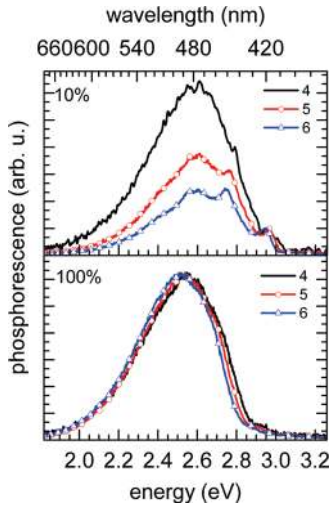

Figure 8. Emission spectra taken at 10 K with a delay time of 500 ns and a gate width of 60 ms for the CF_3-substituted compounds **4**−**6** (a) in a 10 wt % solid-state solution of PMMA and (b) in pure film.The spectra are normalized to unity at the first emission peak.

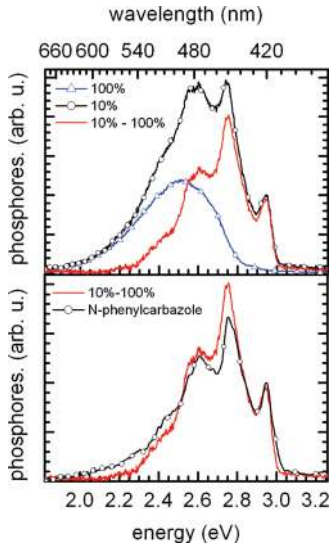

Figure 9. (a) phosphorescence spectra at 10 K of compound **6** in a pure film (blue line) and in a 10 wt % solid-state solution in PMMA (black line), normalized to unity at the first peak of emission, along with the difference spectrum between the pure film spectrum and the solid-state solution spectrum (red line). (b) Comparison of the difference spectrum (red line) with the 10 K phosphorescence spectrum from **7** in a pure film (black line).

and Figure 8a) and when the number of bulky CH_3 groups on the molecule increases. For compound **6**, some vibrational structure is clearly visible in the emission from solid solution, while the luminescence from the neat film contains only the broad feature. We therefore use these two spectra to separate the contributions. Figure 9a shows the emission from the solid-state solution for compound **6**. Also shown is the emission obtained from the neat film, scaled to the red tail of the solid state solution spectrum. Subtracting the scaled neat film spectrum from the solid state solution spectrum results in a well-structured difference spectrum, with a 0−0 peak at 2.95 eV and clear vibrational replica at 2.75, 2.60, and 2.44 eV. In Figure 9b, we compare the so obtained difference spectrum to the phosphorescence spectrum we found for *N*-phenyl-3,6-dimethylcarbazole (**7**) in a neat film. The spectra are very similar. From this analysis it is evident that the emission from compounds **4**−**6** is due to a superposition of the well-structured carbazole phosphorescence with the 0−0 peak at 2.95 eV and a broad unstructured emission centered around 2.5−2.6 eV that we attribute to intermolecular interactions, detailed further as follows. The same applies analogously to **1**−**3**, albeit with a lower contribution by the intermolecular peak in the neat film.

The well-resolved vibrational structure of the phosphorescence in contrast to the broad fluorescence for the CF_3-substituted compounds implies that the state giving rise to phosphorescence is of a different nature from the state causing the fluorescence. This is confirmed by the quantum chemical calculations. The nature of the optical transitions directly affects the position of the associated triplet excited states. The exchange energy, and thus the energy gap between a singlet and the associated triplet state, is well-known to scale with the overlap of the orbitals involved.[32] In consequence, $\pi\rightarrow\pi^*$ transitions result in a larger exchange energy than the charge-transfer-type transitions. For compound **6** this implies that the $\pi\rightarrow\pi^*$ transitions that contribute to S_2 lead to a large calculated singlet−triplet splitting of 0.77 eV, while the charge-transfer-type transitions involved in S_1 give rise to a calculated singlet−triplet splitting of only 0.32 eV (see Figure 6). In consequence, charge-transfer-type transitions cause the second lowest triplet excited state, T_2, while the lowest energy triplet excited state, T_1, has some $\pi-\pi^*$ character that leads to vibrational structure, as in compound **3**.

To summarize the results obtained so far, we find that the CH_3-substituted molecules have a first excited singlet state with 0−0 $S_1\rightarrow S_0$ transition energies are in the range from 3.5 to 3.7 eV, depending on the substituents on the carbazole moiety. Phosphorescence takes place with the 0−0 $T_1\rightarrow S_0$ transition in the range of 2.9−3.0 eV, and it is superimposed by a broad additional emission band. The strong torsion within the biphenyl unit implies that the $\pi-\pi^*$ transition causing the S_1 and T_1 state is localized on the carbazole moieties. As a result, absorption, fluorescence, and phosphorescence are essentially identical to the spectra reported for *N*-arylcarbazoles in the pioneering works by Klöpffer[10−13] and Johnson.[12,18] We have shown this by direct comparison of **1**−**3** to **7**, and by DFT calculations. Our calculations only consider the vertical $S_1\leftarrow S_0$ and $T_1\leftarrow S_0$ transitions. In the excited state, there is likely to be some degree of planarization, yet the similarity between the emission spectra of compounds **1**−**3** and **7** confirms the essentially localized character of the excited states.

When using CF_3 instead of CH_3 for the biphenyl substitution, the absorption and phosphorescence spectra remain very similar, yet the fluorescence shifts to the red and loses all structure. This is because absorption and phosphorescence still involve the $\pi-\pi^*$ transition localized on the carbazole, while fluorescence takes place from an intramolecular charge-transfer (CT) state. Essentially, the result of the CF_3 substitution is to stabilize an unoccupied orbital centered on the biphenyl, so that an intramolecular CT transition from the carbazole to the biphenyl moiety requires less energy than the carbazole-based $\pi-\pi^*$ transition. Without the CF_3 substitution, this order is reversed.

(iii) Excimer Emission. We now consider the broad emission found around 2.5−2.6 eV (Figures 4, 7, and 8) in more detail. First we note that for the spectra taken under steady-state conditions at room temperature (Figure 4), the broad emission is particularly prominent for the CH_3-substituted compound **3**, while it contributes only a little to the spectrum of the CF_3-substituted compound **6**. However, when the emission is recorded at 10 K with a delay time of 500 ns after the excitation pulse and with a long detector gate width of 60 ms (Figures 7 and 8), the broad emission features more strongly in the spectra

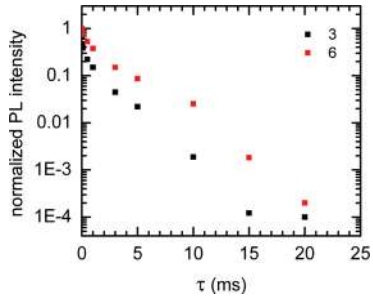

Figure 10. Normalized decay curves of the photoluminescence intensity for compounds **3** and **6** in neat film (where, for example, 1E-3 represents 1×10^{-3}).

of the CF_3-substituted materials. This difference in intensity is easily resolved when considering the detection modes used in more detail. With use of steady-state detection all the photons emitted from an excited state are integrated, so excitations that decay with a high radiative decay rate show up more strongly. Naturally, these excitations have already decayed when waiting for a delay of 500 ns after excitation, and the collected signal intensity is mostly due to excitations with a lower radiative decay rate. Comparison of Figures 4, 7, and 8 suggests therefore that the broad emission centered around 2.5−2.6 eV is present in both classes of materials, yet with a faster decay rate for the CH_3-substituted compounds compared to the CF_3-substituted counterparts. To confirm this hypothesis, we measured the decay time at 2.4 eV in a neat film at room temperature (Figure 10). The emission decays in a non-monomolecular fashion to about $1/e$ of its initial value in 240 μs for **3** yet in 1.2 ms for **6**.

Next we draw attention to the fact that the relative contribution of the broad emission decreases when the molecule has more bulky substituents on the carbazole or when the molecule is diluted into a solid-state solution, suggesting that the broad emission is associated with intermolecular interactions. Furthermore, there is no corresponding absorption feature. We therefore attribute the broad emission to an excimer. We use the term excimer to refer to an intermolecular state that is only stable in the excited state and that has both covalent and ionic contributions to the overall excited-state wave function, Ψ. This can be expressed as

$$\Psi = c_1\Psi(A^*B) + c_2\Psi(AB^*) + c_3\Psi(A^-B^+) + c_4\Psi(A^+B^-) \quad (1)$$

where A and B refer to different molecules, the symbols *, $^+$, and $^-$ indicate the excited or charged state, and c denotes a constant.[32] Usually it is understood that the covalent contribution, given by the first two terms in eq 1, dominate the character of the excited state.

We now consider the subtle differences between the excimer in the CH_3-substituted compounds such as **3** and in the CF_3-substituted ones such as **6**. The energy and shape of the emission are identical, yet, for **6** compared to **3**, the lifetime of the excimer emission is about five times longer and the intensity under steady-state detection is lower. As already mentioned above, this implies a lower radiative decay rate in **6** than in **3**. We interpret this as an indication that the more polar character of a neat film of **6** increases the ionic contribution to the overall excimer wave function expressed in (1). A stronger charge-transfer character of the intermolecular state reduces the wave function overlap that is needed according to Fermi's golden rule to give a high radiative decay rate. The fact that the substitution with the CF_3 group increases the charge-transfer character of the intermolecular excitation is a remarkable detail. The relative amount of the covalent to the ionic contribution in an intermolecular excitation such as an excimer or, in the case of a heterojunction, such as an exciplex is one of the factors that control the efficiency of charge separation at the intermolecular interface.[33,34] It is therefore desirable to be able to fine-tune this property by a simple mechanism such as substitution. From the present data we are not able to differentiate whether the longer lifetime of the excimer is caused by the increased polarity of the two molecules constituting the excimer or whether it can be attributed to the enhanced polarity of the excimer's environment, or both.[35]

We have already shown that the strong torsion in the biphenyl unit in compounds **1**−**6** electronically decouples the two halves of the molecule to some degree, resulting in absorption and phosphorescence spectra that are identical to those of *N*-phenylcarbazole. *N*-Arylcarbazoles and *N*-alkylcarbazoles have been studied extensively in the past by Klöpffer, Johnson, and many others,[11,18−28] and it is well-known that they are prone to form excimers. Given the similar electronic structure, it is instructive to compare the excimer emission we find for compounds **1**−**6** with the existing literature on excimers in *N*-arylcarbazoles and *N*-alkylcarbazoles. These materials can form two different kinds of excimers, depending on their geometric arrangement.

If the carbazoles overlap by only one phenyl ring, a partial overlap excimer is formed. This excimer fluoresces in broad unstructured fashion at about 3.1 eV (400 nm).[19,26] For carbazolophanes that are used as model compounds for the partial overlap excimer, Tani and co-workers[26] also report phosphorescence, though we note that this phosphorescence has vibrational structure with a 0−0 peak about 2.91 eV (425 nm), such as the corresponding *N*-ethylcarbazole monomer. Since the triplet is strongly localized, it is conceivable that the resonance interaction is not sufficient to form a stable triplet excimer. A different conformation is that of a sandwich excimer where the two carbazole derivatives involved overlap fully.[19,26,36] Broad and unstructured fluorescence and phosphorescence are reported centered at about 2.7 eV (460 nm) and at about 2.5 eV (500 nm), respectively, for the sandwich excimer.[19,26,36]

Triplet excimers are not reported often since the singlet−triplet splitting in excimers is small. As a result, triplet excimers are often energetically above the triplet state in the monomer and they become quenched by it.[32] Triplet excimers can be observed if the stabilization energy of the excimer formation is large compared to the S_1-T_1 energy splitting of the monomer, so that the energy level of the excimer triplet is lower than the monomer triplet (Figure 11). For carbazole sandwich excimers, this is the case.[24,26,37] The monomer S_1-T_1 energy splitting is about 0.7 eV (see Figures 2 and 9 for *N*-phenylcarbazole or Figure 3 in ref 26 for *N*-ethylcarbazole). In contrast the energetic stabilization associated with the excimer formation is 0.9 eV, as is evident from the change in S_1 energy from 3.6 to 2.7 eV. We consider that this large stabilization energy is associated with a significant wave function overlap of the π-system in the carbazole sandwich excimer.

If we compare the excimer emission observed in compounds **1**−**6** to the excimer emission reported for *N*-arylcarbazoles and *N*-alkylcarbazoles, we find that our excimer emission centered around 2.5−2.6 eV is energetically identical to the triplet of the carbazole sandwich excimer. Furthermore, the lifetime of the excimer in our compounds is on the order of a few hundred microseconds to milliseconds (Figure 10). This is too long for

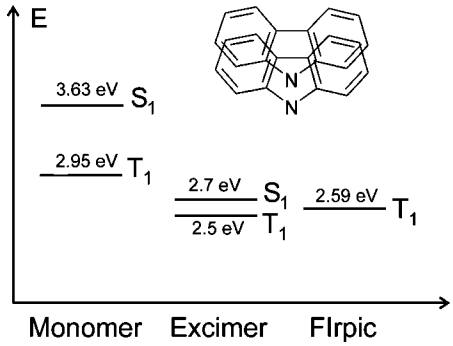

Figure 11. Energy diagram illustrating the singlet and triplet energy levels for the carbazole monomer, for the carbazole excimer, and of the emitter FIrpic.

a singlet excimer, which is typically in the range of tens of nanoseconds,[33,34,38,39] yet it is consistent with a typical phosphorescence lifetime at room temperature for organic solids.[40] On this basis we conclude that the excimer emission observed in compounds **1**−**6** can be assigned to a triplet excimer that is localized on two carbazole moieties in a sandwich configuration. On passing we remind the reader that we attributed the longer lifetime found for the CF_3-substituted **6** to a stronger charge-transfer character of the intermolecular state. This is consistent with reports by Haggquist and co-workers who considered how the balance between geminate pair recombination, triplet excimer formation, and triplet−triplet annihilation in the sandwich excimer of *N*-ethylcarbazole depends on the dielectric constant of the solvent.[36] It also confirms earlier work by Tani et al. on sandwich-type carbazole derivatives[24,26,37] and by Lim et al. on triplet excimers in naphtalene derivatives that arrange in a skewed or L-shaped geometry.[28,41] Both groups pointed out that triplet excimers are stabilized if charge resonance adds to the usual electronic resonance associated with excimers, i.e., if the third and fourth terms in eq 1 also contribute substantially. This is in contrast to singlet excimers, where electronic resonance alone, i.e., the first two terms in eq 1, is often sufficient.

Having established that there is a nonnegligible amount of triplet excimers present in neat films of compounds **1**−**6**, we may now question whether these materials are suitable as hosts for blue triplet emitters. There are a number of reports where compound **1**, that is CDBP, was used as a host for the iridium complex FIrpic. The OLED performance was found to be very good and certainly superior to that with CBP as host material.[7,42] The reason for the good performance of **1** (CDBP) may be that FIrpic has a 0−0 triplet energy of 2.64 eV and the triplet excimer in CDBP is centered around 2.6 eV, i.e., nearly isoenergetic as indicated in Figure 11. The energy-transfer rates for forward transfer and back transfer therefore have to be very similar. Since the lifetime of FIrpic is only in the range of microseconds, whereas the triplet excimer lives for several hundreds of microseconds; this implies that almost all of the excited triplet states still decay from the FIrpic site. To which degree this balance shifts when the energy of the triplet in the phosphorescent emitter is higher than that in the excimer still needs to be investigated in a quantitative fashion.

Summary and Conclusion

We have shown that the substitution on the central biphenyl unit successfully raises the triplet T_1 energy from 2.58 eV in the more planar CBP to 2.95 eV in the twisted compounds **1**−**6**. The monomeric phosphorescence is superimposed by triplet emission centered at 2.6 eV from a sandwich-type excimer localized on the carbazole moiety. This triplet excimer emission can be reduced by increasing the number of bulky substituents on the carbazole. When using CF_3 instead of CH_3 as substituents on the central biphenyl, the fluorescence acquires a charge-transfer character, and the radiative recombination of the triplet excimer reduces. This is attributed to a larger ionic character of the intermolecular triplet excited state for the more polar compounds. It implies that depending on the local molecular polarization, the intermolecular excited state may vary between having a dominant resonance character (more excimer-like) or a stronger coulomb contribution (more charge-transfer-like). A partially similar dependence of the nature of the intermolecular excited state on the local molecular environment has also been observed for molecular heterojunctions, where this effect is known to contribute decisively to the recombination or dissociation rate of excited states.[35] Given the structural similarity of compounds **1**−**6** to the widely used host materials CBP or mCB and the relevant role of long-lived excimer states to device efficiency and lifetime, the possible existence of only weakly emissive triplet excimers from the host materials needs to be taken into account and requires consideration when evaluating the performance of device structures such as WOLEDs.

Acknowledgment. We thank Christian Lennartz for fruitful discussions relating to the DFT calculations. The German−Israeli Foundation is acknowledged for financial support. Support from the Graduiertenkolleg 1640 is gratefully acknowledged.

References and Notes

(1) Hadziioannou, G.; Malliaras, G. *Semiconducting Polymers*; Wiley-VCH: Weinheim, Germany, 2007.
(2) Sun, Y. R.; Giebink, N. C.; Kanno, H.; Ma, B. W.; Thompson, M. E.; Forrest, S. R. *Nature* **2006**, *440*, 908.
(3) Kamtekar, K. T.; Monkman, A. P.; Bryce, M. R. *Adv. Mater.* **2010**, *22*, 572.
(4) Schütz, C.; Hofer, B.; Jaiser, F.; Krueger, H.; Thesen, M.; Janietz, S.; Kohler, A. *Phys. Status Solidi B* **2008**, *245*, 810.
(5) D'Andrade, B. W.; Brooks, J.; Adamovich, V.; Thompson, M. E.; Forrest, S. R. *Adv. Mater.* **2002**, *14*, 1032.
(6) Su, S. J.; Sasabe, H.; Takeda, T.; Kido, J. *Chem. Mater.* **2008**, *20*, 1691.
(7) Tanaka, I.; Tabata, Y.; Tokito, S. *Chem. Phys. Lett.* **2004**, *400*, 86.
(8) van Dijken, A.; Bastiaansen, J. J. A. M.; Kiggen, N. M. M.; Langeveld, B. M. W.; Rothe, C.; Monkman, A.; Bach, I.; Stossel, P.; Brunner, K. *J. Am. Chem. Soc.* **2004**, *126*, 7718.
(9) Brunner, K.; van Dijken, A.; Borner, H.; Bastiaansen, J. J. A. M.; Kiggen, N. M. M.; Langeveld, B. M. W. *J. Am. Chem. Soc.* **2004**, *126*, 6035.
(10) Klöpffer, W. *Ber. Bunsen-Ges.* **1969**, *73*, 864.
(11) Klöpffer, W.; Fischer, D. *J. Polym. Sci., Polym. Symp.* **1973**, *40*, 43.
(12) Klöpffer, W. *ACS Symp. Ser.* **1987**, *358*, 264.
(13) Rippen, G.; Kaufmann, G.; Klöpffer, W. *Chem. Phys.* **1980**, *52*, 165.
(14) Itaya, A.; Okamoto, K. I.; Kusabayashi, S. *Bull. Chem. Soc. Jpn.* **1976**, *49*, 2037.
(15) Vala, M. T.; Haebig, J.; Rice, S. A. *J. Chem. Phys.* **1965**, *43*, 886.
(16) Adachi, C.; Forrest, S. R.; Thompson, M. E. *New J. Chem.* **2002**, *26*, 1171.
(17) Schrögel, P.; Tomkeviciene, A.; Strohriegl, P.; Hoffmann, S. T.; Köhler, A.; Lennartz, C. *J. Mater. Chem.* **2011**, DOI: 10.1039/c0jm03321a.
(18) Johnson, P. C.; Offen, H. W. *J. Chem. Phys.* **1971**, *55*, 2945.
(19) Qian, L.; Bera, D.; Holloway, P. H. *J. Chem. Phys.* **2007**, *127*, 244707.
(20) Williams, E. L.; Haavisto, K.; Li, J.; Jabbour, G. E. *Adv. Mater.* **2007**, *19*, 197.
(21) Burkhart, R. D.; Jhon, N. I.; Boileau, S. *Macromolecules* **1991**, *24*, 6310.
(22) Abia, A. A.; Burkhart, R. D. *Macromolecules* **1984**, *17*, 2739.
(23) Katayama, H.; Hisada, K.; Yanagida, M.; Ohmori, S.; Ito, S.; Yamamoto, M. *Thin Solid Films* **1993**, *224*, 253.
(24) Benten, H.; Guo, J.; Ohkita, H.; Ito, S.; Yamamoto, M.; Sakumoto, N.; Hori, K.; Tohda, Y.; Tani, K. *J. Phys. Chem. B* **2007**, *111*, 10905.

(25) Shimizu, H.; Kakinoya, Y.; Takehira, K.; Yoshihara, T.; Tobita, S.; Nakamura, Y.; Nishimura, J. *Bull. Chem. Soc. Jpn.* **2009**, *82*, 860.
(26) Tani, K.; Tohda, Y.; Takemura, H.; Ohkita, H.; Ito, S.; Yamamoto, M. *Chem. Commun. (Cambridge, U.K.)* **2001**, *19*, 1914.
(27) Cai, J. J.; Lim, E. C. *J. Chem. Phys.* **1992**, *97*, 3892.
(28) Cai, J. J.; Lim, E. C. *J. Phys. Chem.* **1994**, *98*, 2515.
(29) Becke, A. D. *J. Chem. Phys.* **1993**, *98*, 5648.
(30) Lee, C. T.; Yang, W. T.; Parr, R. G. *Phys. Rev. B* **1988**, *37*, 785.
(31) Kasha, M. *Discuss. Faraday Soc.* **1950**, *9*, 14.
(32) Köhler, A.; Bässler, H. *Mater. Sci. Eng., R* **2009**, *66*, 71.
(33) Morteani, A. C.; Sreearunothai, P.; Herz, L. M.; Friend, R. H.; Silva, C. *Phys. Rev. Lett.* **2004**, *92*, 247402.
(34) Veldman, D.; Ipek, O.; Meskers, S. C. J.; Sweelssen, J.; Koetse, M. M.; Veenstra, S. C.; Kroon, J. M.; van Bavel, S. S.; Loos, J.; Janssen, R. A. J. *J. Am. Chem. Soc.* **2008**, *130*, 7721.
(35) Huang, Y. S.; Westenhoff, S.; Avilov, I.; Sreearunothai, P.; Hodgkiss, J. M.; Deleener, C.; Friend, R. H.; Beljonne, D. *Nat. Mater.* **2008**, *7*, 483.
(36) Haggquist, G. W.; Burkhart, R. D. *J. Phys. Chem.* **1993**, *97*, 2576.
(37) Tani, K.; Yamamoto, S.; Kubono, K.; Hori, K.; Tohda, Y.; Takemura, H.; Nakamura, Y.; Nishimura, J.; Benten, H.; Ohkita, H.; Ito, S.; Yamamoto, M. *Chem. Lett.* **2007**, *36*, 460.
(38) Winnik, F. M. *Chem. Rev.* **1993**, *93*, 587.
(39) Yin, C.; Schubert, M.; Bange, S.; Stiller, B.; Castellani, M.; Neher, D.; Kumke, M.; Hörhold, H. H. *J. Phys. Chem. C* **2008**, *112*, 14607.
(40) Turro, N. J. *Modern Molecular Photochemistry*: University Science Books: Sausalito, CA, 1991.
(41) Lim, E. C. *Acc. Chem. Res.* **1987**, *20*, 8.
(42) Tokito, S.; Iijima, T.; Tsuzuki, T.; Sato, F. *Appl. Phys. Lett.* **2003**, *83*, 2459.

JP107408E